The Bioscan AN INTERNATIONAL QUARTERLY JOURNAL OF LIFE SCIENCES 21(2): S.I (2), 21230-21245, 2026 www.thebioscan.com

Exploring the Therapeutic Potential of Daidzein in Polycystic Ovary Syndrome Using Network Pharmacology and Molecular Modeling

Shweta Myagadeyavar[1], Namit Kudatarkar*[2] , Vishal S. Patil[3] , Sachin Gudasi[4]

[1]Department of Pharmacology, KLE College of Pharmacy, Belagavi, KLE Academy of Higher Education and Research, Belagavi, Karnataka, India.
Email: shwetamyagadeyavar@gmail.com
ORCID ID - https://orcid.org/009-0009-4851-731X
[2*]Assistant Professor, Department of Pharmacology, KLE College of Pharmacy, Belagavi, KLE Academy of Higher Education and Research, Belagavi, Karnataka, India.
Email: namitkudatarkar18@gmail.com
Phone: 9552880153
ORCID ID- https://orcid.org/0000-0002-1535-5117
[3]Assistant Professor, Department of Pharmacology, KLE College of Pharmacy, Belagavi, KLE Academy of Higher Education and Research, Belagavi, Karnataka, India
ORCID ID: https://orcid.org/0000-0002-1219-1962
[4]Department of Pharmacognosy, KLE College of Pharmacy, Belagavi, KLE Academy of Higher Education and Research Belagavi, Karnataka, India
ORCID ID: https://orcid.org/0000-0002-4173-2967

Corresponding Author: Namit Kudatarkar, namitkudatarkar18@gmail.com
DOI: https://doi.org/10.63001/tbs.2026.v21.i02.S.I(2).pp21230-21245

KEYWORDS
Daidzein, molecular docking, network pharmacology, ADMET, polycystic ovary syndrome.

Received on:
01/06/2026
Revised on:
09/06/2026
Accepted on:
18/06/2026
Published on:
28/06/2026

Abstract

Polycystic ovary syndrome (PCOS) is a heterogeneous endocrine and metabolic disorder characterized by hyperandrogenism, ovulatory dysfunction, insulin resistance, and chronic low-grade inflammation. Despite the availability of several therapeutic strategies, most current interventions primarily provide symptomatic relief and may be associated with adverse effects or limited long-term efficacy. These limitations highlight the need for safer and more effective multi-target therapeutic agents. Daidzein, a naturally occurring soy isoflavone, exhibits antioxidant, anti-inflammatory, estrogenic, and insulin-sensitizing properties, suggesting potential therapeutic relevance in PCOS.

The present study employed an integrated in silico approach comprising network pharmacology, molecular docking, molecular dynamics simulation, and ADMET profiling to investigate the therapeutic potential of daidzein against PCOS. Daidzein-associated targets were retrieved from the Comparative Toxicogenomics Database, while PCOS-related genes were obtained from the GeneCards database. Shared targets were subsequently analyzed using protein–protein interaction network construction, Gene Ontology enrichment, and KEGG pathway analyses. Key proteins were further evaluated through molecular docking and molecular dynamics simulation.

A total of 76 overlapping targets were identified. Network analysis recognized TP53, ESR1, IL6, TNF, EGFR, and MAPK3 as major hub proteins. Functional enrichment analyses demonstrated significant involvement of PI3K-Akt, MAPK, TNF, NF-κB, IL-17, and estrogen signaling pathways. Molecular docking revealed favorable binding affinities of daidzein toward ESR1, CYP19A1, and AKT1, while molecular dynamics simulation confirmed stable interaction of the CYP19A1-daidzein complex throughout the simulation period. ADMET prediction indicated favorable intestinal absorption, acceptable drug-likeness, and an overall favorable pharmacokinetic profile. Overall, these findings of the present study indicate that daidzein may possess therapeutic potential in PCOS through multi-target modulation of key molecular pathways, thereby warranting further experimental validation.

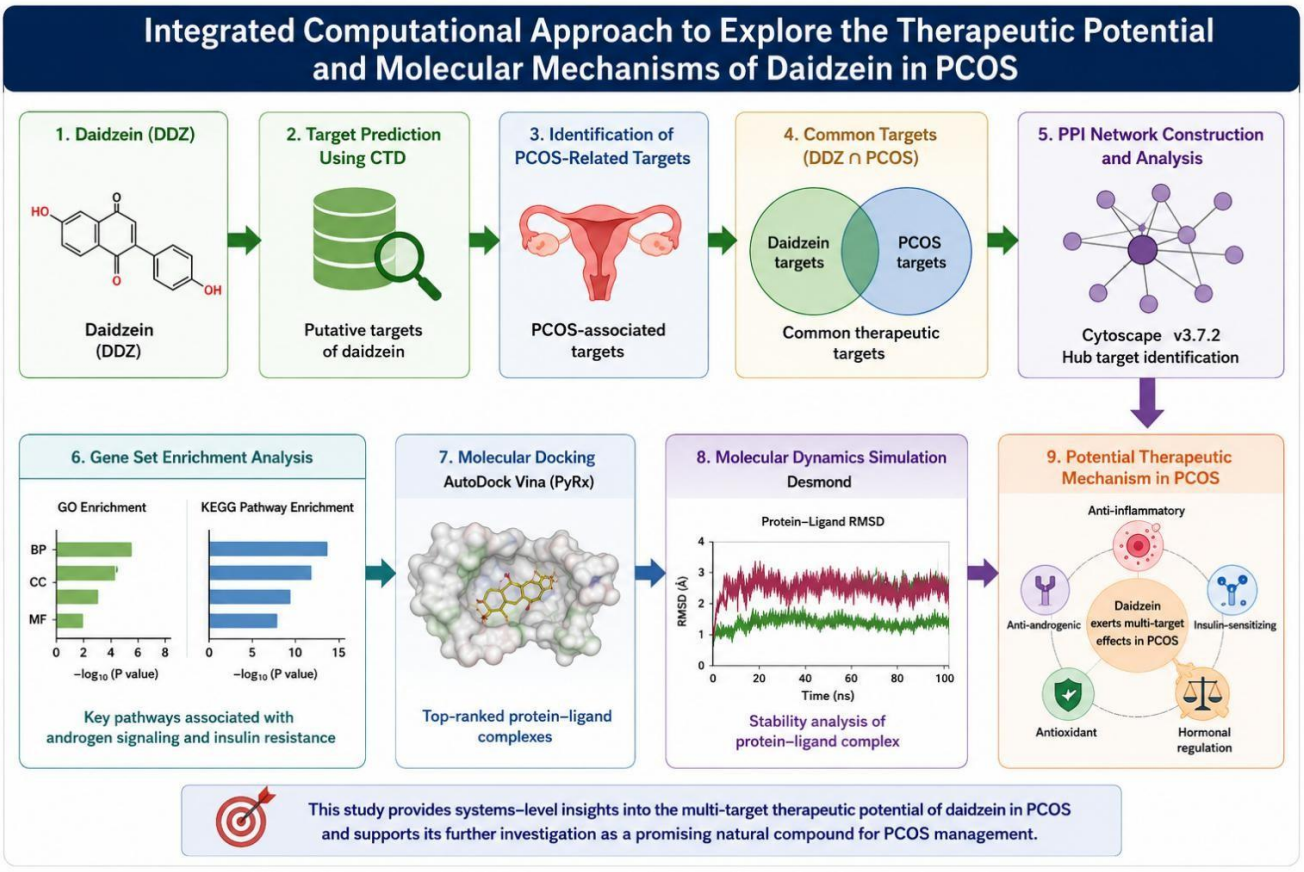

Graphical Abstract: Integrated computational workflow illustrating the therapeutic potential of daidzein (DDZ) in polycystic ovary syndrome (PCOS). The schematic summarizes target prediction, network pharmacology, protein–protein interaction analysis, enrichment studies, molecular docking, and molecular dynamics simulations. The multi-target mechanisms identified include anti-inflammatory, insulin-sensitizing, hormonal regulation, antioxidant, and anti-androgenic effects.

1.INTRODUCTION

Polycystic ovary syndrome (PCOS) is among the most prevalent endocrine and metabolic disorders affecting women of reproductive age worldwide, with an estimated global prevalence ranging from 6% to 20% depending on the diagnostic criteria employed.[1] The syndrome is characterized by hyperandrogenism, ovulatory dysfunction, polycystic ovarian morphology, insulin resistance, and chronic low-grade inflammatory status.[2] In addition to reproductive abnormalities, women affected by PCOS are predisposed to several long-term metabolic and systemic complications, including obesity, type 2 diabetes mellitus, cardiovascular disorders, and endometrial abnormalities.[24]

The pathophysiology of PCOS is multifactorial and involves complex interactions among endocrine, metabolic, inflammatory, and genetic factors.[4] Insulin resistance is considered a key contributor to the progression of PCOS, as it enhances ovarian androgen synthesis and disrupts normal follicular development.[5] Aberrant activation of signaling cascades such as PI3K-Akt and MAPK is implicated in impaired insulin signaling, chronic inflammation, and ovarian dysfunction associated with PCOS.[3,9] Increased expression of pro-inflammatory cytokines, including TNF-α and IL-6, further worsens the metabolic and reproductive abnormalities observed in the disorder.[7]

Current therapeutic approaches mainly focus on symptomatic management using agents such as metformin, letrozole, clomiphene citrate, oral contraceptives, and anti-androgens.[8] However, these therapies may produce adverse effects and often fail to target the complex and multifaceted pathophysiology of the disorder.[9] Therefore, increasing attention has been directed toward plant-derived bioactive compounds possessing multi-target pharmacological activities and comparatively favorable safety profiles.[10]

Daidzein, a naturally occurring soy isoflavone, has demonstrated antioxidant, anti-inflammatory, estrogenic, and insulin-sensitizing properties in several experimental studies.[11,54] These pharmacological activities suggest its possible therapeutic relevance in PCOS. However, the precise molecular mechanisms underlying its action against PCOS remain insufficiently understood.

The integration of network pharmacology with molecular docking and molecular dynamics simulation provides a systems-level approach for exploring the multi-target therapeutic interactions of bioactive compounds.[12] Accordingly, the present study was designed to elucidate the potential molecular mechanisms of daidzein in PCOS through a comprehensive computational strategy incorporating network pharmacology, molecular docking, molecular dynamics simulation, and ADMET evaluation.

2.MATERIALS & METHODS

Study design

The present study employed an integrated in silico approach comprising network pharmacology, protein-protein interaction (PPI) analysis, functional enrichment analysis, molecular docking, molecular dynamics (MD)

simulation, and ADMET profiling to assess the potential therapeutic significance of daidzein in PCOS.

Retrieval of daidzein structure

The 2D chemical molecular structure of daidzein was retrieved from the PubChem database in Structure Data File (SDF) format and standardized for downstream computational analyses.[13] Protein targets associated with daidzein were obtained from the Comparative Toxicogenomics Database (CTD).[14] All retrieved targets were pooled and deduplicated to derive a final set of non-duplicated targets.[15]

Identification of PCOS-associated genes

PCOS- correlated genes were retrieved from the GeneCards database using the search term 'polycystic ovary syndrome'. Entries with higher relevance scores (>20), reflecting stronger evidence of disease association, were retained for analysis.[16]

Identification of shared targets

Daidzein targets and PCOS genes were cross-referenced using Venn diagram-based intersection analysis to identify shared targets. These overlapping genes were considered as candidates through which daidzein may exert its effects in PCOS and were subsequently used for PPI network construction and pathway enrichment analysis.[17]

3. ADMET AND DRUG-LIKENESS EVALUATION

Prediction strategy

Pharmacokinetic and toxicity properties of daidzein were assessed using the ADMETlab 3.0 web server, which applies validated machine-learning models across multiple ADMET endpoints. The compound was submitted in SMILES format, and predictions were generated for absorption, distribution, metabolism, excretion, and toxicity parameters.[18]

Absorption and bioavailability

Intestinal absorption was evaluated using Caco-2 permeability (3.21) and human intestinal absorption (HIA) probability (0.99), both pointing to excellent oral uptake.[19] The blood–brain barrier (BBB) permeability score of 0.64 suggests a moderate likelihood of CNS exposure.[20] Taken together, the data support high oral bioavailability with partial central nervous system penetration potential.[21]

Distribution

4. MOLECULAR DOCKING STUDIES

The predicted steady-state volume of distribution (log VDss) was −0.21, consistent with limited tissue distribution.[22] Plasma protein binding (PPB) was high at 91.8%, with a fraction unbound (Fu) of 11.9%, indicating that strong protein binding restricts free drug availability.[23] Formulation strategies aimed at enhancing systemic exposure may therefore be warranted.[24]

Metabolic profiling

Daidzein was predicted to be a substrate for CYP3A4 (0.99), CYP2D6 (0.99), and CYP2C9 (0.99).[25] Inhibition probabilities across these isoforms were low (below 0.4), suggesting limited potential for drug–drug interactions.[26] The compound therefore carries metabolic liability as a CYP substrate but poses minimal risk as an inhibitor.[27]

Toxicological evaluation

Consensus model predictions indicate non-mutagenicity (Ames test probability: 0.77) and borderline carcinogenicity (0.47).[28] The acute oral LD_{50} was estimated at 512 mg/kg, placing daidzein in the moderate acute toxicity range.[29] Low predicted probabilities for hepatotoxicity and nephrotoxicity indicate limited liver and kidney toxicity concerns, although moderate acute toxicity and borderline carcinogenicity predictions warrant further investigation.[30] (Daidzein's ADMET profile; Supplementary Table S2).

Taken together, these parameters confirm that daidzein possesses a balanced physicochemical profile, meeting key drug-likeness filters while maintaining favorable ADMET properties.

Drug-likeness evaluation

Daidzein satisfied Lipinski's Rule of Five (compound molecular weight 254.24 g/mol, logP 2.3, hydrogen bond donor count of 2 and hydrogen bond acceptor count of 4), indicating favorable oral drug-likeness. Veber's criteria were also met, with a topological polar surface area (TPSA) value of 66 Å2 and only 2 rotatable bonds, supporting good bioavailability potential. The estimated bioavailability score was 0.55, indicating moderate oral bioavailability. In addition, the synthetic accessibility score was 3.1, suggesting that daidzein is chemically tractable and feasible for synthesis.[31]

Protein-Protein Interaction and MCODE Cluster Analysis

The identified targets were uploaded to the STRING database for construction of a protein–protein interaction network restricted to Homo sapiens, applying a high-confidence interaction threshold. Isolated nodes were excluded to improve network specificity. The generated network was subsequently visualized and evaluated using Cytoscape software, where degree-based topological parameters were determined to identify the key hub proteins. The MCODE plugin was subsequently applied under default settings to detect densely connected functional clusters, which were analyzed for their biological relevance to PCOS pathophysiology.[32]

Interaction Network Construction

A compound-associated target–pathway network was assembled in Cytoscape v3.10.1 by importing and merging compound–target and target–pathway datasets. Within the network, nodes represent daidzein, its predicted protein targets, and associated signaling pathways; edges reflect the interactions among them. The Network Analyzer tool was used for topological analysis. Nodes were ranked by degree to identify highly connected hub candidates, while edges were ranked by betweenness centrality to pinpoint interactions central to information flow within the network. Betweenness centrality values for individual nodes were also evaluated to distinguish hub and bottleneck proteins. This multi-parameter network analysis was used to infer the key targets and pathways through which daidzein may act in PCOS.[33]

Preparation of Ligand and Protein

The structural coordinates of daidzein (DDZ) were retrieved in SDF format from PubChem.13,10 The ligand was imported into PyRx (AutoDock Vina interface), processed into docking-compatible PDBQT files were processed into docking-compatible PDBQT files, and energy minimized using default Vina Wizard parameters prior to docking studies.17, The lowest-energy conformer was selected for docking studies. Crystal structures of human therapeutic targets relevant to PCOS pathophysiology, namely CYP19A1/aromatase (PDB IDs: 4KQ8 and 3S79) and ESR1 (PDB ID: 2IOK), were downloaded from the RCSB Protein Data Bank.[34, 31]

Assessment of Active Site Residues

The human CYP19A1 (aromatase) crystal structure in complex with 4-androstene-3,17-dione and dithionite at the heme center (deposited in the Protein Data Bank as 4KQ8 ; 2.91 Å resolution), expressed in Spodoptera

frugiperda (Sf21) insect cells, was employed for molecular docking analysis relevant to PCOS-associated steroidogenic dysregulation. Key active-site residues include ARG435 and THR310, which contribute to catalytic ligand recognition, while ILE133, PHE134, and MET374 help form the hydrophobic substrate access channel. The heme prosthetic group is anchored through the conserved axial ligand CYS437. These residues are commonly evaluated in inhibitor docking studies aimed at modulating estrogen biosynthesis. In addition, potential ligand-binding pockets were predicted using the PrankWeb server.[35, 36]

Protein-Ligand Docking Analysis

Docking analysis was carried out to determine the binding affinity of daidzein (DDZ) with CYP19A1 and ESR1 using PyRx (v0.8), integrated with Open Babel (v3.1) and AutoDock Vina.[37] Ligand structures were subjected to energy minimization using the MMFF94 force field and subsequently prepared in PDBQT format for docking analysis for docking compatibility.[38] Protein structures (PDB IDs: 4KQ8 and 2IOK) were downloaded from the RCSB Protein Data Bank followed by deletion of crystallographic water molecules and non-essential heteroatoms, after incorporation of polar hydrogen atoms and partial atomic charges were assigned using the Gasteiger method , the structures were saved in PDBQT format for molecular docking.34 Docking was carried out using the Vina Wizard in PyRx. The active-site grid box for CYP19A1 was centered at X = 84.0005, Y = 50.7928, Z = 46.7683 with dimensions of 61.6003 × 70.4823 × 50.7157 Å, while for ESR1 it was centered at X = 37.2155, Y = 18.1418, Z = 39.3272 with dimensions of 42.7330 × 53.2880 × 49.8372 Å. Conformational sampling was optimized by setting the exhaustiveness parameter to 8. Binding affinities were estimated using the AutoDock Vina scoring function, and docking poses were ranked based on binding energy.37 The most stable complexes were selected for interaction analysis using BIOVIA Discovery Studio Visualizer 2019, identifying hydrogen bonds, hydrophobic, and π-π interactions.[39] Although RMSD-based redocking validation was not performed because the study focused on comparative binding prioritization and downstream molecular dynamics analysis, the docking protocol followed widely accepted AutoDock Vina workflows reported in the literature. This limitation should be considered when interpreting docking scores. Therefore, complex selection was based on Gibbs free binding energy and the consistency of protein–ligand interaction patterns rather than docking pose revalidation.

Protein-Ligand Molecular Dynamics Analysis

Using the Desmond simulation package integrated within Schrödinger, MD simulations were performed to examine the binding stability, structural dynamics, and conformational flexibility of daidzein in complex with human CYP19A1 (PDB ID: 4KQ8). The protein–ligand complex was initially energy-minimized using the OPLS_2005 force field. The prepared system was embedded in an orthorhombic simulation box under periodic boundary conditions and solvated using the TIP3P water model with a 10 Å spacing from the protein to the box edges. Sodium and chloride ions were introduced to neutralize the system and maintain physiological ionic strength at 0.15 M NaCl.

After solvation, the system underwent energy minimization followed by equilibration using the Desmond relaxation protocol under NVT and NPT equilibration ensembles with positional restraints applied to the protein–ligand complex on heavy atoms. Following system equilibration, a 100 ns molecular dynamics production run was executed under constant pressure and temperature (NPT) conditions maintained at 300 K and 1 atm using the predefined Desmond simulation protocol. The generated simulation trajectories were further analyzed through parameters such as root mean square deviation (RMSD), root mean square fluctuation (RMSF), and protein–ligand interaction mapping to investigate conformational stability, amino acid flexibility, and the durability of intermolecular interactions in the CYP19A1–daidzein complex.[40]

Determining potential targets

A total of 177 daidzein related targets were obtained from the Comparative Toxicogenomics Database (CTD). associated targets were retrieved from the Comparative Toxicogenomics Database (CTD), while 1,207 polycystic ovary syndrome (PCOS)-related genes were obtained from GeneCards. Venn diagram analysis identified 76 overlapping targets between the two datasets, representing potential key genes through which daidzein may exert therapeutic effects in PCOS (Fig. 2); Supplementary Table S1.

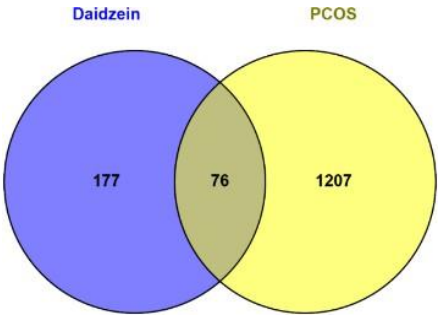

Fig. 2. Overlapping targets between daidzein and polycystic ovary syndrome.

A network of protein-protein interactions

PPI network analysis and MCODE cluster mapping point to a multitarget mechanism for daidzein in PCOS, spanning inflammatory, endocrine, metabolic, and apoptotic regulatory nodes (Fig. 3). The full PPI network comprised 76 nodes and 1,009 edges, with TP53 and ESR1 (degree = 56) emerging as the most connected hubs. Their centrality reflects the critical involvement of cell-cycle control, apoptosis, genomic stability, and estrogen-mediated transcription in PCOS pathobiology. IL6, TNF, EGFR, MAPK3, MYC, and JUN were also prominent, suggesting that daidzein attenuates chronic low-grade inflammation, abnormal ovarian cell proliferation, and insulin resistance through coordinated effects on MAPK, NF-κB, and growth factor signaling. BCL2 and CASP3 nodes indicate modulation of the balance between cell survival and programmed death in ovarian tissue.

MCODE Cluster Analysis

MCODE analysis identified a high-density core cluster (Cluster 1; score = 32.895) comprising 39 genes central to hormone receptor signaling (ESR1, ESR2, AR, PGR, PPARG), inflammatory mediators (IL1A, IL1B, IL6, TNF, NFKB1), cell-cycle and apoptosis regulators (CCND1, CDK4, CDKN1A, TP53, CASP3, BCL2), and key signaling kinases (MAPK1, MAPK3, EGFR, IGF1R). This cluster captures the primary mechanistic axis through which daidzein may regulate ovarian function and metabolic homeostasis. A secondary cluster (Cluster 2; score = 5) included xenobiotic-metabolizing enzymes (UGT1A1, UGT1A7, UGT1A8, UGT1A10, CYP1B1), reflecting a complementary detoxification and steroid metabolism module that may contribute to hormonal balance and reduce oxidative burden **(Table 1).**

5. RESULTS AND DISCUSSIONS

Table 1. MCODE cluster analysis of overlapping targets.

Clusters	Score	Nodes	Edges
Cluster 1	32.895	39	625
Cluster 2	5	5	10

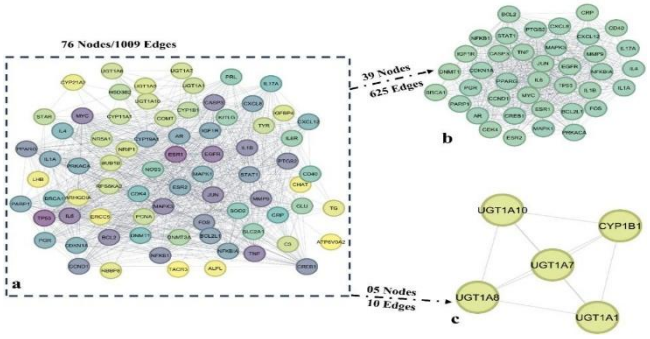

Fig. 3. (a) Full protein-protein interaction (PPI) network showing 76 nodes and 1,009 edges; (b) MCODE Cluster 1 showing a densely connected signaling module enriched with TP53, IL6, EGFR, MYC, AR, ESR1, BCL2, STAT1, and TNF; (c) MCODE Cluster 2 showing a metabolic enzyme-associated module containing UGT1A1, UGT1A7, UGT1A8, UGT1A10, and CYP1B1. Green nodes represent signaling hub proteins, while yellow-green nodes indicate metabolic enzymes. Edges represent experimentally validated or computationally predicted interactions.

6. GENE ONTOLOGY ENRICHMENT ANALYSIS

Gene Ontology enrichment analysis demonstrated that the overlapping targets were mainly associated with inflammatory regulation, cellular stress responses, apoptosis, metabolic regulation, and hormone-mediated signaling pathways relevant to PCOS pathophysiology (Fig. 4). Biological process analysis highlighted genes involved in cellular response to stimuli, inflammatory signaling, oxidative stress regulation, and lipid metabolism, suggesting the potential role of daidzein in modulating metabolic and inflammatory disturbances associated with PCOS. Cellular component analysis indicated significant enrichment of intracellular organelles, endoplasmic reticulum, chromatin-associated complexes, and membrane-associated regions involved in receptor-mediated signaling and steroidogenesis. Molecular function analysis predominantly identified protein binding, transcription factor interaction, and regulatory signaling activities associated with endocrine regulation, insulin signaling, and ovarian function. Collectively, the enrichment findings suggest that daidzein may exert therapeutic effects through coordinated modulation of inflammatory, metabolic, and hormonal pathways involved in PCOS progression.

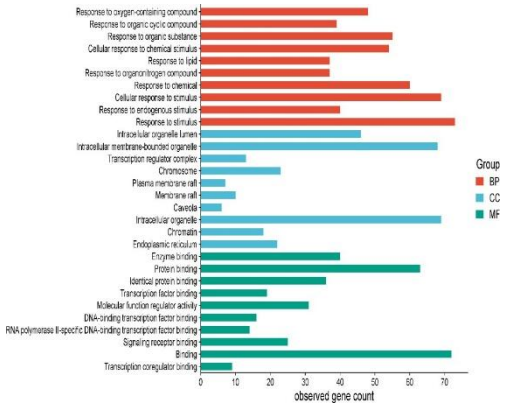

Fig. 4. Gene ontology enrichment analysis of common targets.

6. DAIDZEIN-TARGET-PATHWAY NETWORK

The compound–target–pathway network was developed in Cytoscape v3.10.1 by importing interaction datasets and applying Network Analyzer for topological characterization (Fig. 5). Nodes were ranked by degree and edges by betweenness centrality. The PI3K-Akt signaling pathway was the most strongly enriched, with 20 connected targets including BRCA1, CDK4, MAPK1, NOS3, CDKN1A, MAPK3, CREB1, IGF1R, CCND1, PRL, BCL2, NFKB1, KITLG, EGFR, IL6R, IL4, BCL2L1, IL6, MYC, and TP53 — collectively involved in insulin signaling, glucose metabolism, follicular development, granulosa cell proliferation, apoptosis, and inflammatory responses. The MAPK signaling pathway (20 edges) was equally enriched, pointing to roles in steroidogenesis, cell-cycle regulation, and ovarian remodeling. IL-17 (15 edges) and TNF signaling (13 edges) pathways were also prominent, as was the estrogen signaling pathway (13 edges), consistent with the hormonal dysregulation characteristic of PCOS.

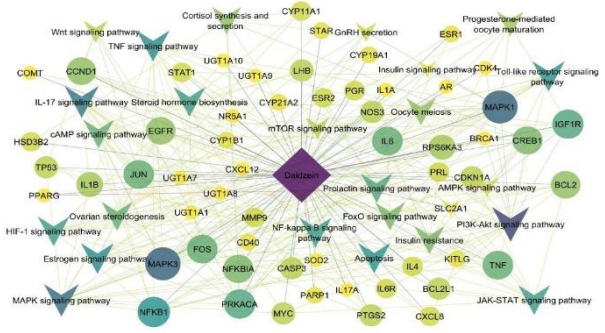

Fig. 5. Compound-target-pathway interaction network of daidzein against polycystic ovary syndrome. The purple diamond represents daidzein; circular nodes represent target genes/proteins; triangular nodes represent enriched signaling pathways. Yellow nodes indicate metabolic enzymes, green nodes indicate inflammatory mediators, and blue nodes indicate hormone- and growth-related hub proteins. Edges represent experimentally validated or computationally predicted interactions.

7. KEGG PATHWAY ENRICHMENT ANALYSIS

Endocrine and reproductive regulation is represented by steroid hormone biosynthesis (hsa00140), ovarian steroidogenesis (hsa04913), estrogen signaling (hsa04915), prolactin signaling (hsa04917), GnRH signaling (hsa04912), progesterone-mediated oocyte maturation (hsa04914), oocyte meiosis (hsa04114), and cortisol synthesis and secretion (hsa04927). These pathways involve steroidogenic enzymes (CYP11A1, CYP19A1, HSD3B2, CYP21A2), nuclear hormone receptors (ESR1/ESR2, PGR, AR), and gonadotropic regulators (LHB, PRKACA). Additional enrichment in apoptosis (hsa04210), HIF-1 signaling (hsa04066), JAK-STAT signaling (hsa04630), and Wnt signaling (hsa04310) reflects involvement in cell survival, hypoxia response, cytokine signaling, and follicular development.

KEGG enrichment analysis identifies interconnected regulation across inflammatory, metabolic, endocrine, and cell survival networks in the context of PCOS therapy (Fig. 6). Inflammatory pathways, including IL-17 signaling (hsa04657), TNF signaling (hsa04668), NF-κB signaling (hsa04064), and Toll-like receptor signaling (hsa04620), are significantly enriched, pointing to attenuation of low-grade chronic inflammation through MAPK1/3, NFKB1/NFKBIA, IL6, IL1B, TNF, CXCL8, and MMP9. Central metabolic and survival pathways, including PI3K-Akt (hsa04151), MAPK signaling (hsa04010), mTOR signaling (hsa04150), FoxO signaling (hsa04068), AMPK signaling (hsa04152), and insulin signaling (hsa04910), collectively indicate improvement in of insulin sensitivity, glucose uptake, and energy balance via IGF1R, EGFR, CCND1, CREB1, BCL2, CDKN1A, and RPS6KA3.

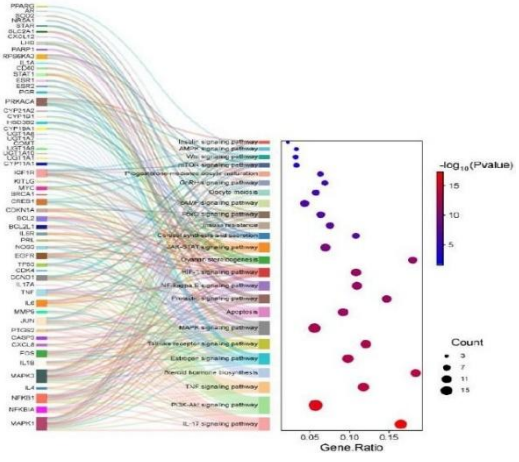

Fig. 6. KEGG Pathway enrichment analysis of common targets.

8. MOLECULAR DOCKING

Active Site Residues by van der Waals forces.

This interaction pattern within the ligand-binding pocket is consistent with phytoestrogenic behavior.Against CYP19A1 (4KQ8), daidzein scored −8.3 kcal/mol, forming Based on PDB records, the active site of CYP19A1 (PDB ID: 4KQ8) encompassed ARG A:115, ILE A:132, ILE A:133, LEU A:152, ALA A:306, MET A:303, CYS A:437, GLY A:439, and ALA A:438. Predicted active site residues from PrankWeb are summarized in Table S4 (Supplementary Material). For ESR1 (PDB ID: 2IOK), active site residues from PDB entries included GLU B:1353, PHE B:1404, LEU B:1391, LEU B:1387, MET B:1388, MET B:1421, and ILE B:1424.

PrankWeb-predicted residues are listed in Table S5 (Supplementary Material). Docking analyses integrated both the predicted active site data and published literature evidence.

Ligand-Protein Docking

Daidzein (DDZ) showed strong binding to three key PCOS-relevant targets: estrogen receptor-α (ESR1; PDB ID: 2IOK), aromatase (CYP19A1; PDB ID: 4KQ8), and AKT1 (PDB ID: 3S79), supporting potential regulatory activity across estrogen signaling, steroidogenesis, and insulin resistance pathways. Against ESR1 (2IOK), daidzein achieved a docking score of −8.8 kcal/mol, forming a hydrogen bond with GLU B:1353, a π–π interaction with PHE B:1404, and hydrophobic π-alkyl contacts with LEU B:1387, LEU B:1391, MET B:1388, ILE B:1424, and MET B:1421, further stabilized four hydrogen bonds with ARG A:115, ILE A:132, GLY A:439, and CYS A:437, a π-sigma interaction with ILE A:133, a π-sulfur contact with MET A:303, and additional hydrophobic contacts with ALA A:306, LEU A:152, and ALA A:438. These interactions suggest stable accommodation within the steroid-binding cavity and indicate possible modulation of androgen-to-estrogen conversion. For AKT1 (3S79), daidzein demonstrated a binding energy of −7.7 kcal/mol, with hydrogen bonds at LYS A:440 and GLN A:428, π–π stacking with TYR A:361, and hydrophobic contacts with PRO A:429, PHE A:427, PHE A:418, VAL A:422, and TYR A:424, consistent with modulation of the PI3K–Akt pathway.

For comparison, metformin showed considerably weaker binding to CYP19A1 (−4.7 kcal/mol), forming only two hydrogen bonds with ALA A:151 and MET A:276, with limited additional contacts. The higher interaction density, broader hydrogen-bonding pattern, and more favorable binding energies of daidzein across ESR1, CYP19A1, and AKT1 collectively support its capacity to address both the endocrine and metabolic dimensions of PCOS simultaneously.

Table 2. Prioritized protein target binding affinities for DDZ and Metformin

Ligand	PubChem ID	Target	BE (kcal/mol)	Total Interactions	Active Sites	HBI	Non-HBI
Daidzein (DDZ)	5281708	2IOK (ESR1 - Estrogen Receptor-α)	−8.8	9	9	GLU:1353	PHE:1404, LEU:1387, LEU:1391, MET:1388, ILE:1424, MET:1421
Daidzein (DDZ)	5281708	4KQ8 (CYP19A1-Aromatase)	−8.3	10	10	ARG:115, ILE:132, GLY:439, CYS:437	ILE:133, MET:303, ALA:306, LEU:152, ALA:438
Daidzein (DDZ)	5281708	3S79 (CYP19A1-Aromatase)	−7.7	9	9	LYS:440, GLN:428	TYR:361, PRO:429, PHE:427, PHE:418, VAL:422, TYR:424
Metformin	4091	4KQ8 (CYP19A1-Aromatase)	−4.7	4	4	ALA:151, MET:276	LEU:202, PHE:203

(AS: Active Sites; HBI: hydrogen bond interactions; Non-HBI: non-hydrogen bond interactions; Van der Waals, π-alkyl, π-cation, π-sigma, π-π stacked, π-π T-shaped interactions; BE: Binding Energy.)

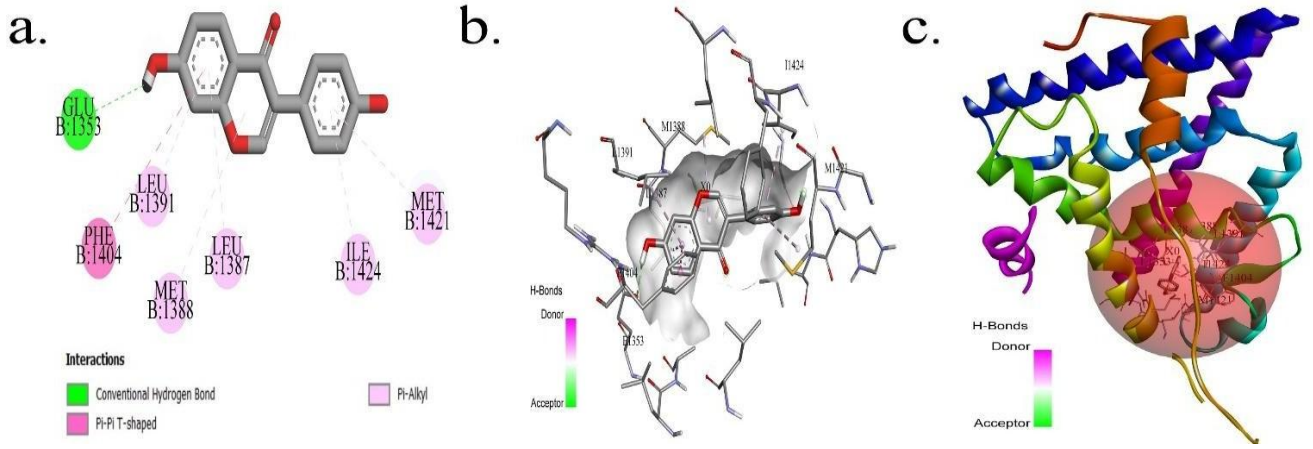

Fig. 7. (a) 2IOK (ESR1) 2D interaction diagram; (b) 3D binding pose; (c) 3D pose with binding pocket.

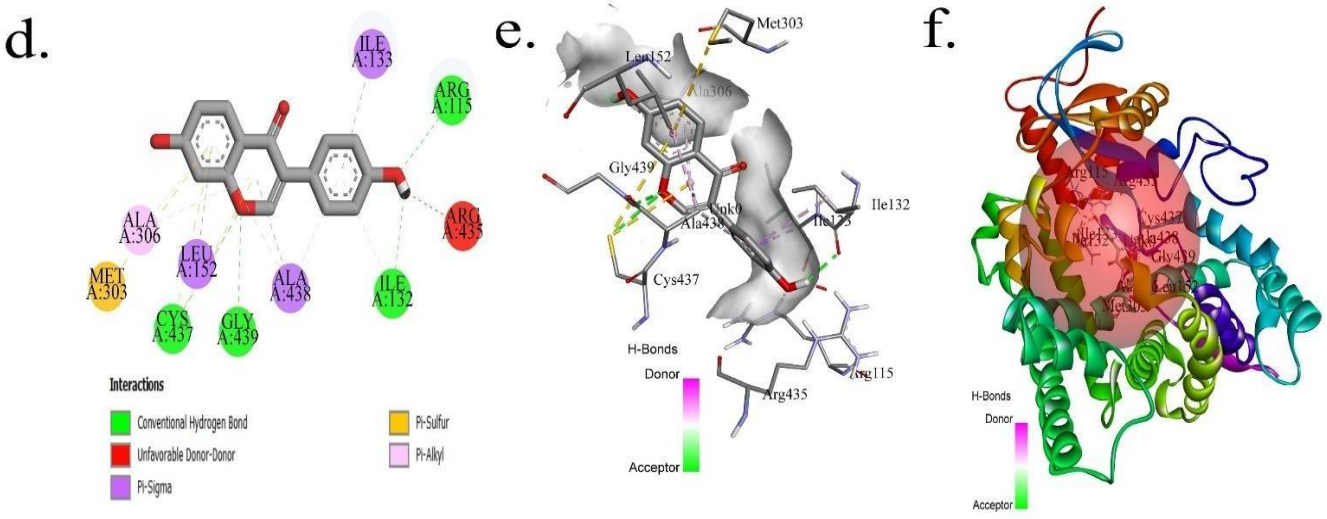

Fig. 8. (d) 4KQ8 (CYP19A1) 2D interaction diagram; (e) 3D binding pose; (f) 3D pose with binding pocket.

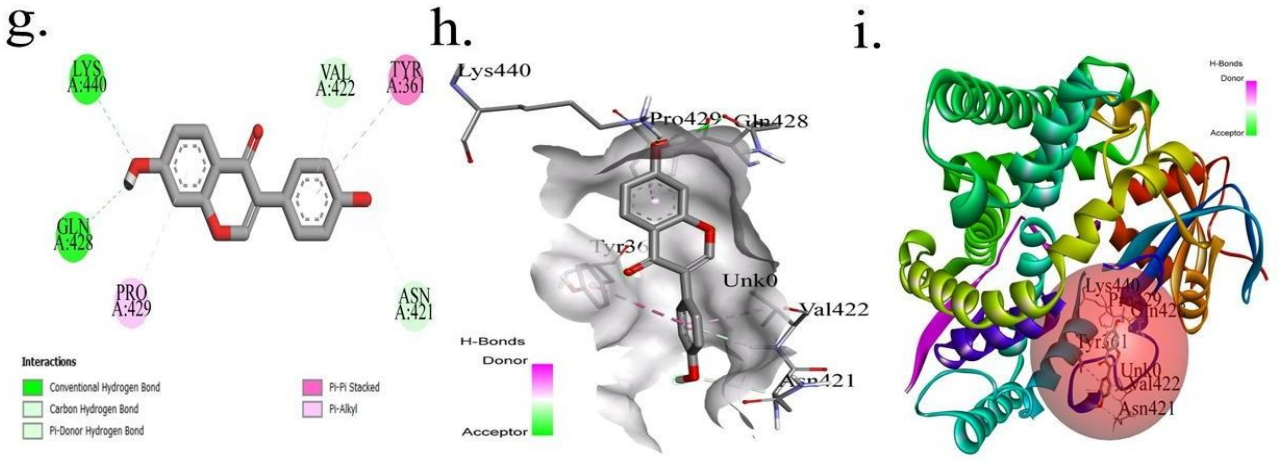

Fig. 9. (g) 3S79 (CYP19A1) 2D interaction diagram; (h) 3D binding pose; (i) 3D pose with binding pocket.

9. MOLECULAR DYNAMICS SIMULATIONS OF THE 4KQ8-DAIDZEIN COMPLEX

modest residue-level fluctuations (average 3.689 Å), and the ligand RMSF was low at 1.637 Å, suggesting that daidzein remained well positioned within the binding site throughout the simulation.

A 100 ns MD simulation was conducted with the Desmond package in the Schrödinger Suite to evaluate the stability, conformational dynamics, and sustained binding of daidzein within the 4KQ8 active site. The protein-ligand complex was energy-minimized under the OPLS_2005 force field, embedded in an orthorhombic TIP3P water box with a minimum 10 Å buffer from protein to box boundary, and neutralized with Na^+ and Cl^- ions with a physiological ionic strength of 0.15 M NaCl. Following energy minimization and equilibration under the standard Desmond NVT/NPT relaxation protocol, the production MD was conducted at 300 K and 1 atm using the NPT ensemble.

After equilibration, the 4KQ8-daidzein complex reached stable Cα and backbone RMSD plateaus of 2.643 ± 0.217 Å and 2.437 ± 0.738 Å, respectively, indicating that no major conformational transitions occurred during production dynamics. Protein RMSF analysis showed

Ligand-protein contact analysis revealed a persistent and cooperative interaction network. Binding is primarily driven by hydrogen bonds and water-mediated contacts, supplemented by hydrophobic and π-cation interactions. The carbonyl oxygen of daidzein forms a strong water-bridged hydrogen bond with ARG435 (181% interaction persistence, indicating multiple concurrent contacts), reinforced by a water bridge to SER114 (72% occupancy). On the opposite phenyl ring, the phenolic hydroxyl engages ARG375 through water-mediated hydrogen bonds at occupancies of 107% and 34%. Additional water-mediated contacts with PHE432 (35%) and TRP141 (40%) contribute to ligand stabilization through solvent-assisted positioning. A π-cation interaction between the aromatic ring of daidzein and ARG115 (38% persistence) provides electrostatic anchoring within the pocket. Taken together, residues ARG375, ARG435, SER114, PHE432, and GLU439 maintain binding geometry and interaction continuity, while hydrophobic contributions from TRP141, ILE132, and neighboring residues complete the enclosure of the ligand. This interaction profile suggests stable accommodation and favorable binding dynamics of daidzein within the 4KQ8 active site.

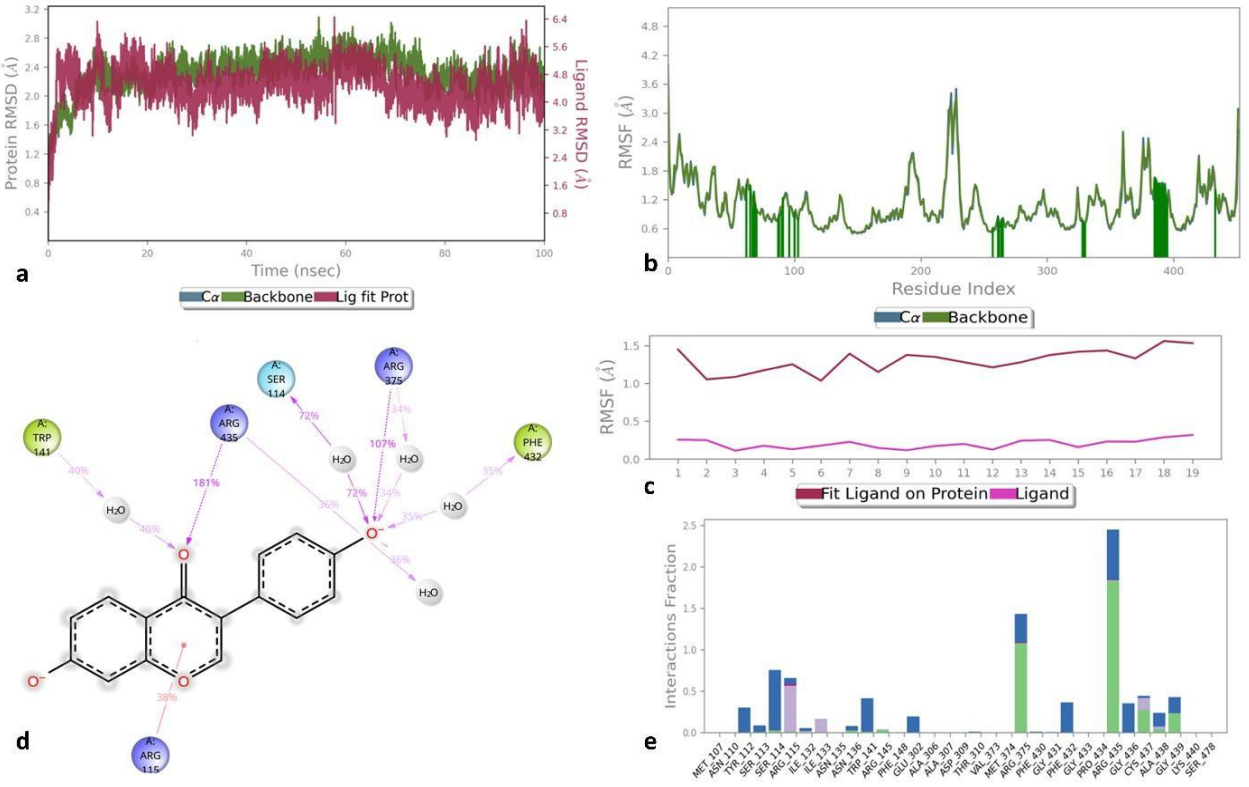

Fig. 10. (a) Protein ligand RMSD plot of 4KQ8-daidzein complex, (b) Protein RMS Plot, (c) Ligand RMSF plot, (d) ligand protein contact of daidzein with the respective amino acids of the 4KQ8 protein, (e) Protein ligand contacts of 4KQ8-daidzein complex with the respective amino acids.

10. DISCUSSION

PCOS is a multifactorial disorder involving endocrine imbalance, insulin resistance, oxidative stress, and chronic inflammation.[41,48] Increasing evidence supports the importance of multi-target therapeutic strategies for effective management of the disorder.[42]

The present study identified multiple overlapping targets between daidzein and PCOS-associated genes, supporting the hypothesis that daidzein may modulate interconnected endocrine and inflammatory pathways. Hub proteins such as ESR1, IL6, TNF, TP53, and AKT1 are strongly associated with ovarian dysfunction, insulin resistance, and inflammatory progression in PCOS.[43,49,56]

Pathway enrichment analysis revealed considerable participation of PI3K-Akt, MAPK, NF-κB, and estrogen signaling pathways, indicating possible regulation of insulin sensitivity, steroidogenesis, follicular

development, and inflammatory responses.[3,44,57] Inflammatory signaling pathways including TNF and IL-17 further support the role of chronic inflammation in disease progression.[50,53]

Molecular docking demonstrated favorable binding interactions of daidzein with ESR1, CYP19A1, and AKT1, suggesting potential modulation of estrogen receptor signaling and metabolic pathways. These findings are in line with prior reports describing the anti-inflammatory and insulin-sensitizing effects of daidzein.[54]

Molecular dynamics modelling added to the stability of the CYP19A1–daidzein complex under dynamic conditions.[46] Computational ADMET analysis also suggested acceptable drug-likeness and favorable pharmacokinetic behavior, although additional experimental validation remains necessary.

Overall, the integrated computational findings suggest that daidzein may exert therapeutic effects through simultaneous modulation of multiple endocrine, metabolic, and inflammatory pathways.

11. CONCLUSION

The present in silico investigation suggests that daidzein may possess potential therapeutic relevance in the management of polycystic ovary syndrome through multi-target modulation of key endocrine, metabolic, and inflammatory pathways. Network pharmacology, molecular docking, molecular dynamics simulation, and ADMET analyses collectively support its possible interaction with critical regulatory proteins associated with PCOS pathophysiology. Although the findings provide important computational insights into the mechanistic potential of daidzein, experimental validation through in vitro and in vivo investigations is required to confirm its biological and therapeutic utility.

11. REFERENCES

1. Bozdag G, Mumusoglu S, Zengin D, Karabulut E, Yildiz BO. The prevalence and phenotypic features of polycystic ovary syndrome: A systematic review and meta-analysis. Human Reproduction. 2016;31(12):28 41-2855. doi:10.1093/humrep/dew218
2. Chang KJ, Chen JH, Chen KH. The pathophysiological mechanism and clinical treatment of polycystic ovary syndrome: A molecular and cellular review of the literature. International Journal of Molecular Sciences. 2024;25(16):9037. doi:10.3390/ijms25169037
3. Li T, Mo H, Chen W, Li L, Xiao Y, Zhang J, Li X, Lu Y. Role of the PI3K-Akt signaling pathway in the pathogenesis of polycystic ovary syndrome. Reproductive Sciences. 2017;24(5):646-655. doi:10.1177/1933719116667606
4. Diamanti-Kandarakis E, Dunaif A. Insulin resistance and the polycystic ovary syndrome revisited: An update on mechanisms and implications. Endocrine Reviews. 2012;33(6):981-1030. doi:10.1210/er.2011-1034
5. Qu X, Donnelly R. Sex hormone-binding globulin (SHBG) as an early biomarker and therapeutic target in polycystic ovary syndrome. International Journal of Molecular Sciences. 2020;21(21):8191. doi:10.3390/ijms21218191
6. Cheng T, Wu Y, Zhang L, Yu Y. Insulin resistance, autophagy and apoptosis in patients with polycystic ovary syndrome: Association with PI3K signaling pathway. Frontiers in Endocrinology. 2022;13:1091147. doi:10.3389/fendo.2022.1091147
7. Rudnicka E, Suchta K, Grymowicz M, Calik-Ksepka A, Smolarczyk K, Duszewska AM, Smolarczyk R, Meczekalski B. Chronic low-grade inflammation in pathogenesis of PCOS. International Journal of Molecular Sciences. 2021;22(7):3789. doi:10.3390/ijms22073789
8. Legro RS, Arslanian SA, Ehrmann DA, Hoeger KM, Murad MH, Pasquali R, Welt CK. Diagnosis and treatment of polycystic ovary syndrome: An Endocrine Society clinical practice guideline. Journal of Clinical Endocrinology and Metabolism. 2013;98(12):4565-4592. doi:10.1210/jc.2013-2350
9. Wang K, Li Y. Signaling pathways and targeted therapeutic strategies for polycystic ovary syndrome. Frontiers in Endocrinology. 2023;14:1191759. doi:10.3389/fendo.2023.1191759
10. Chavez GN, Jaworsky K, Basu A. The effects of plant-derived phytochemical compounds and phytochemical-rich diets on females with polycystic ovarian syndrome: A scoping review of clinical trials. International Journal of Environmental Research and Public Health. 2023;20(15):6534. doi:10.3390/ijerph20156534
11. Tan Y, Zhang X, Cheang WS. Isoflavones daidzin and daidzein inhibit lipopolysaccharide-induced inflammation in RAW264.7 macrophages. Chinese Medicine. 2022;17(1):95. doi:10.1186/s13020-022-00660-7
12. Salo-Ahen OMH, Alanko I, Bhadane R, Bonvin AMJJ, Honorato RV, Hossain S, Juffer AH, Kabedev A, Lahtela-Kakkonen M, Larsen AS, Lescrinier E. Molecular dynamics simulations in drug discovery and pharmaceutical development. Processes. 2021;9(1):71. doi:10.3390/pr9010071
13. Kim S, Chen J, Cheng T, Gindulyte A, He J, He S, Li Q, Shoemaker BA, Thiessen PA, Yu B, Zaslavsky L. PubChem 2025 update. Nucleic Acids Research. 2025;53(D1):D1516-D1525. doi:10.1093/nar/gkae1059
14. Davis AP, Grondin CJ, Johnson RJ, Sciaky D, Wiegers J, Wiegers TC, Mattingly CJ. Comparative Toxicogenomics Database (CTD): Update 2021. Nucleic Acids Research. 2021;49(D1):D1138-D1143. doi:10.1093/nar/gkaa891
15. Kudatarkar N, Jalalpure S, Patil VS, Kurangi B. System biology and chemoinformatics approaches to decode the molecular mechanisms of chrysin against colon cancer. Journal of Applied Pharmaceutical Science. 2021;11(9):57-65. doi:10.7324/JAPS.2021.110907
16. Fishilevich S, Barshir R, Iny-Stein T, Zelig O, Guan-Golan Y, Safran M, Lancet D. Disease interpretation of non-coding genomic elements with the GeneCards Suite. Molecular Genetics and Metabolism. 2021;132(S1):S123. doi:10.1016/j.ymgme.2020.12.299
17. Kondapuram SK, Sarvagalla S, Coumar MS. Docking-based virtual screening using PyRx Tool: Autophagy target Vps34 as a case study. In: Roy K, editor. Molecular Docking for Computer-Aided Drug Design. London: Academic Press; 2021. p.463-477. doi:10.1016/B978-0-12-822312-3.00014-4
18. Fu L, Shi S, Yi J, Wang N, He Y, Wu Z, Peng J, Deng Y, Wang W, Wu C, Lyu A. ADMETlab 3.0: An updated comprehensive online ADMET prediction platform enhanced with broader coverage, improved performance, API functionality and decision support. Nucleic Acids Research. 2024;52(W1):W422-W431. doi:10.1093/nar/gkae266
19. Porter CJH, Trevaskis NL, Charman WN. Lipids and lipid-based formulations: Optimizing the oral delivery of lipophilic drugs. Nature Reviews Drug Discovery. 2007;6(3):231-248. doi:10.1038/nrd2197
20. Pires DEV, Blundell TL, Ascher DB. pkCSM: Predicting small-molecule pharmacokinetic and toxicity properties using graph-based signatures. Journal of Medicinal Chemistry. 2015;58(9):4066-4072. doi:10.1021/acs.jmedchem.5b00104
21. Yang H, Lou C, Sun L, Li J, Cai Y, Wang Z, Li W, Liu G, Tang Y. admetSAR 2.0: Web-service for prediction and optimization of chemical ADMET properties. Bioinformatics. 2019;35(6):1067-1069. doi:10.1093/bioinformatics/bty707.
22. Daina A, Michielin O, Zoete V. SwissADME: A free web tool to evaluate pharmacokinetics, drug-likeness and

medicinal chemistry friendliness of small molecules. Scientific Reports. 2017;7(1):42717. doi:10.1038/srep42717.
23. Smith DA, Di L, Kerns EH. The effect of plasma protein binding on in vivo efficacy: Misconceptions in drug discovery. Nature Reviews Drug Discovery. 2010;9(12):929-939. doi:10.1038/nrd3287.
24. Wekker V, Van Dammen L, Koning A, Heida KY, Painter RC, Limpens J, Laven JSE, Roeters van Lennep JE, Roseboom TJ, Hoek A. Long-term cardiometabolic disease risk in women with PCOS: A systematic review and meta-analysis. Human Reproduction Update. 2020;26(6):942-960. doi:10.1093/humupd/dmaa029.
25. Zanger UM, Schwab M. Cytochrome P450 enzymes in drug metabolism: Regulation of gene expression, enzyme activities, and impact of genetic variation. Pharmacology and Therapeutics. 2013;138(1): 103-141. doi:10.1016/j.pharmthera.2012.12.007.
26. Guengerich FP. Human cytochrome P450 enzymes. In: Ortiz de Montellano PR, ed. Cytochrome P450: Structure, Mechanism, and Biochemistry. Cham: Springer; 2015:523-785. doi:10.1007/978-3-319-12108-6_10.
27. Patel S. Polycystic ovary syndrome (PCOS), an inflammatory, systemic, lifestyle endocrinopathy. Journal of Steroid Biochemistry and Molecular Biology. 2018;182:27-36. doi:10.1016/j.jsbmb.2018.04.008.
28. Zhang J, Li H, Zhang Y, Huang J, Ren L, Zhang C, Zou Q, Zhang Y. Computational toxicology in drug discovery: Applications of artificial intelligence in ADMET and toxicity prediction. Briefings in Bioinformatics. 2025;26(5):bbaf533. doi:10.1093/bib/bbaf533.
29. OECD. Test No. 423: Acute Oral Toxicity – Acute Toxic Class Method. OECD Guidelines for the Testing of Chemicals, Section 4. Paris: OECD Publishing; 2002. doi:10.1787/9789264071001-en.
30. Shinde SS, Giram PS, Wakte PS, Bhusari SS. ADMET tools in the digital era: Applications and limitations. In: Advances in Pharmacology. Vol 103. London: Academic Press; 2025:65-80. doi:10.1016/bs.apha.2024.10.003.
31. Desaipatti R, Kudatarkar N, Gudasi S. In silico screening and experimental validation of Carissa carandas L. extract against cyclophosphamide-induced cardiotoxicity in Wistar rats. Journal of Applied Pharmaceutical Science. 2025;15(3):248-259. doi:10.7324/JAPS.2025.198181.
32. Yu G, Wang LG, Han Y, He QY. clusterProfiler: An R package for comparing biological themes among gene clusters. OMICS: A Journal of Integrative Biology. 2012;16(5):284-287. doi:10.1089/omi.2011.0118.
33. Gudasi S, Kumar D, Tewari S, Kavalapure RS, Ranade SD. Decoding the molecular mechanism via systems biology-based insights into neoschaftoside from Ailanthus altissima targeting lung cancer. Scientific Reports. 2026;16:3328. doi:10.1038/s41598-025-33214-0.
34. Kouranov A, Xie L, de la Cruz J, Chen L, Westbrook J, Bourne PE, Berman HM. The RCSB PDB information portal for structural genomics. Nucleic Acids Research. 2006;34(Suppl 1):D302-D305. doi:10.1093/nar/gkj067.
35. Huang B. MetaPocket: A meta approach to improve protein ligand binding site prediction. OMICS: A Journal of Integrative Biology. 2009;13(4):325-330. doi:10.1089/omi.2009.0045.
36. Morris GM, Huey R, Lindstrom W, Sanner MF, Belew RK, Goodsell DS, Olson AJ. AutoDock4 and AutoDockTools4: Automated docking with selective receptor flexibility. Journal of Computational Chemistry. 2009;30(16):2785-2791. doi:10.1002/jcc.21256.
37. Trott O, Olson AJ. AutoDock Vina: Improving the speed and accuracy of docking with a new scoring function, efficient optimization, and multithreading. Journal of Computational Chemistry. 2010;31(2):455-461. doi:10.1002/jcc.21334.
38. Halgren TA. Merck molecular force field. I. Basis, form, scope, parameterization, and performance of MMFF94. Journal of Computational Chemistry. 1996;17(5-6):490-519. doi:10.1002/(SICI)1096-987X(199604)17:5/6<490::AID-JCC1>3.0.CO;2-P.
39. Baroroh U, Muscifa ZS, Destiarani W, Rohmatullah FG, Yusuf M. Molecular interaction analysis and visualization of protein-ligand docking using BIOVIA Discovery Studio Visualizer. Indonesian Journal of Computational Biology. 2023;2(1):22-30. doi:10.24252/ijcb.v2i1.40178.
40. Berendsen HJC, Postma JPM, van Gunsteren WF, DiNola A, Haak JR. Molecular dynamics with coupling to an external bath. Journal of Chemical Physics. 1984;81(8):3684-3690. doi:10.1063/1.448118.
41. Shorakae S, Ranasinha S, Abell S, Lambert G, Lambert E, de Courten B, Teede H. Inter-related effects of insulin resistance, hyperandrogenism, sympathetic dysfunction and chronic inflammation in PCOS. Clinical Endocrinology. 2018;89(5):628-633. doi:10.1111/cen.13808.
42. Bai X, Tang Y, Li Q, Liu D, Liu G, Fan X, Liu Z, Yu S, Tang T, Wang S, Li L. An integrated analysis of network pharmacology, molecular docking, and experiment validation to explore the new candidate active component and mechanism of Cuscutae Semen-Mori Fructus coupled-herbs in treating oligoasthenozoospermia. Drug Design, Development and Therapy. 2021;15:2059-2089. doi:10.2147/DDDT.S303964.
43. De Leo V, Musacchio MC, Cappelli V, Massaro MG, Morgante G, Petraglia F. Genetic, hormonal and metabolic aspects of PCOS: An update. Reproductive Biology and Endocrinology. 2016;14(1):38. doi:10.1186/s12958-016-0173-x.
44. González F, Rote NS, Minium J, Kirwan JP. Increased activation of nuclear factor κB triggers inflammation and insulin resistance in polycystic ovary syndrome. Journal of Clinical Endocrinology and Metabolism. 2006;91(4):1508-1512. doi:10.1210/jc.2005-2327.
45. Azziz R, Carmina E, Chen Z, Dunaif A, Laven JSE, Legro RS, Lizneva D, Natterson-Horowtiz B, Teede HJ, Yildiz BO. Polycystic ovary syndrome. Nature Reviews Disease Primers. 2016;2:16057. doi:10.1038/nrdp.2016.57.
46. Gudasi S, Patil MB, Gharge S, Ranade SD, Fanai HL, Chand J, Ahmad SF, Attia SM, Emran TB. Exploring the anti-obesity potential of Ailanthus excelsa Roxb in vitro enzymatic inhibition and computational pharmacology insights. Scientific Reports. 2025;15(1):32747. doi:10.1038/s41598-025-32747-8.
47. Hollingsworth SA, Dror RO. Molecular dynamics simulation for all. Neuron. 2018;99(6):1129-1143. doi:10.1016/j.neuron.2018.08.011.
48. Hospital A, Goñi JR, Orozco M, Gelpí JL. Molecular dynamics simulations: Advances and applications. Advances and Applications in Bioinformatics and Chemistry. 2015;8:37-47. doi:10.2147/AABC.S70333.
49. Armanini D, Boscaro M, Bordin L, Sabbadin C. Controversies in the pathogenesis, diagnosis and treatment of PCOS: Focus on insulin resistance, inflammation, and hyperandrogenism. International Journal of Molecular Sciences. 2022;23(8):4110. doi:10.3390/ijms23084110.
50. Bansal B, Kishore AT, Kathiresan S, Ghachi AF, Pradhan S, Paul S, Chaturvedi K, Singh M, Patil S, Johnson LS, Akshay VP, NS D, Pillai A. A systematic review of inflammatory markers in polycystic ovary syndrome (PCOS) and meta-analysis of interleukin-6 (IL-6) in case-control studies. Cureus. 2025;17(4):e82350. doi:10.7759/cureus.82350.

51. Escobar-Morreale HF. Polycystic ovary syndrome: Definition, aetiology, diagnosis and treatment. Nature Reviews Endocrinology.2018;14(5):270-284. doi:10.1038/nrendo.2018.24.
52. Jorgensen WL, Chandrasekhar J, Madura JD, Impey RW, Klein ML. Comparison of simple potential functions for simulating liquid water. Journal of Chemical Physics. 1983;79(2):926-935. doi:10.1063/1.445869.
53. Peebles E, Mahalingaiah S. Environmental exposures and polycystic ovary syndrome: A review. Seminars in Reproductive Medicine. 2024;42(4):253-273. doi:10.1055/s-0044-1786996.
54. Popovic M, Sartorius G, Christ-Crain M. Chronic low-grade inflammation in polycystic ovary syndrome: Is there a (patho)-physiological role for interleukin-1? Seminars in Immunopathology. 2019;41(4):447-459. doi:10.1007/s00281-019-00737-4.
55. Sakamoto Y, Kanatsu J, Toh M, Naka A, Kondo K, Iida K. The dietary isoflavone daidzein reduces expression of pro-inflammatory genes through PPARα/γ and JNK pathways in adipocyte and macrophage co-cultures. PLOS ONE. 2016;11(2):e0149676. doi:10.1371/journal.pone.0149676.
56. Stelzer G, Rosen N, Plaschkes I, Zimmerman S, Twik M, Fishilevich S, Stein TI, Nudel R, Lieder I, Mazor Y, Kaplan S. The GeneCards Suite: From gene data mining to disease genome sequence analyses. Current Protocols in Bioinformatics. 2016;54(1):1.30.1-1.30.33. doi:10.1002/cpbi.5.
57. Wang J, Yin T, Liu S. Dysregulation of immune response in PCOS organ system. Frontiers in Immunology. 2023;14:1169232. doi:10.3389/fimmu.2023.1169232.
58. Wang Y, Yang J, Wang Y, Chen Y, Wang Y, Kuang H, Feng X. Upregulation of TXNIP contributes to granulosa cell dysfunction in polycystic ovary syndrome via activation of the NLRP3 inflammasome. Molecular and Cellular Endocrinology. 2023;561:111824. doi:10.1016/j.mce.2022.111824.

Funding

This research did not receive any specific grant from funding agencies in the public, commercial, or not-for-profit sectors.

CRediT authorship contribution statement:

- Manuscript writing, software, methodology, computational studies, data curation and data analysis: Shweta Myagadeyavar, Sachin Gudasi, Vishal S. Patil
- Supervision, writing – review & editing: Namit Kudatarkar

Acknowledgments:

The authors are very thankful to Principal Dr. S. S. Jalalpure and Head of the Department of Pharmacology KLE College of Pharmacy, Belagavi for their support and guidance and for providing computational facilities and institutional resources needed to complete the research. We also thank colleagues from the Departments of Pharmacology for their valuable discussions and technical assistance.

Declaration of Conflict of Interest

The authors declare that there is no conflict of interest associated with this work.

Ethical Approval

Not applicable, as the present study is entirely based on computational and in silico methodologies.

Data availability

All datasets generated or analysed during this study are included in this article and its supplementary information section.

Supplementary data

Table S1. Overlapping genes

OVERLAPPING GENES						
ALPL						
AR						
ARHGDIA						
ATP6V0A2						
BCL2						
BCL2L1						
BRCA1						
BUB1B						
C3						

Table S2. Daidzein's ADMET profile

Parameter	Predicted Value	Interpretation

Absorption	Caco-2: 3.21; HIA: 0.99	Excellent intestinal absorption; high oral bioavailability
BBB Permeability	0.64	Moderate CNS penetration potential
Distribution	logVDss: −0.21; PPB: 91.8%; Fu: 11.9%	Restricted tissue distribution due to strong plasma protein binding
Metabolism	CYP3A4: 0.99; CYP2D6: 0.99; CYP2C9: 0.99	Substrate for major CYP isoforms; inhibition probabilities low (<0.4)
Cardiotoxicity (hERG)	hERG inhibition (10 μM): 0.09; overall risk: 0.59	Low direct cardiotoxicity risk; moderate overall probability warrants monitoring
Mutagenicity (Ames)	0.77	Non-mutagenic
Carcinogenicity	0.47	Borderline probability; requires validation
Acute oral toxicity (LD_{50})	512 mg/kg	Moderate acute toxicity
Other toxicities	Hepatotoxicity/nephrotoxicity: low	Favorable safety margin

Table S3. Complete gene composition of MCODE clusters.

Clusters	Genes
Cluster 1	AR, BCL2, BCL2L1, BRCA1, CASP3, CCND1, CD40, CDK4, CDKN1A, CREB1, CRP, CXCL12, CXCL8, DNMT1, EGFR, ESR1, ESR2, FOS, IGF1R, IL17A, IL1A, IL1B, IL4, IL6, JUN, MAPK1, MAPK3, MMP9, MYC, NFKB1, NFKBIA, PARP1, PGR, PPARG, PRKACA, PTGS2, STAT1, TNF, TP53,
Cluster 2	UGT1A10, UGT1A7, UGT1A8, UGT1A1, CYP1B1

Table S4: Active site residue predicted from Prank web (4KQ8)

Name	rank	score	probability	Sas points	Surf atoms	Center x	Center y	Center z	Residue ids
pocket1	1	47.93	0.974	174	86	85.8322	50.2053	44.0151	A_115 A_132 A_133 A_134 A_141 A_145
									A_148 A_152 A_199 A_203 A_221 A_224 A_302 A_303 A_306 A_307 A_309 A_310 A_311 A_314 A_364 A_369 A_370 A_372 A_373 A_374 A_375 A_429 A_430 A_435 A_436 A_437 A_438 A_439 A_442 A_443 A_446 A_477 A_478
Pocket2	2	4.26	0.188	43	23	75.9942	48.6993	35.3004	A_357 A_361 A_422 A_424 A_427 A_428 A_429 A_430 A_440 A_441 A_444

Table S5. Active site residue predicted from prank web (2IOK)

Name	Rank	Score	Probability	Sas point	Surf atom	Center x	Center y	Center z	Residue ids
Pocket1	1	23.62	0.874	88	56	17.9756	35.475	51.64	A_343 A_346 A_347 A_349 A_350 A_353 A_383 A_384 A_387 A_388 A_391 A_404 A_418 A_419 A_420 A_421 A_424 A_428 A_521 A_524 A_525 A_528
Pocket2	2	21.67	0.855	91	53	37.3657	14.1326	51.452	B_1343 B_1346 B_1347 B_1350 B_1353 B_1383
									B_1384 B_1387 B_1388 B_1391 B_1394 B_1404 B_1418 B_1419 B_1420 B_1421 B_1424 B_1428 B_1521 B_1524 B_1525

Pocket3	3	7.92	0.464	79	35	32.9645	29.6667	46.7163	A_427 A_513 A_516 A_520 A_523 B_1377 B_1380 B_1381 B_1456 B_1457 B_1459 B_1460 B_1515 B_1518 B_1519 B_1522 B_1526
Pocket4	4	6.55	0.36	65	36	20.7152	19.2254	49.5055	A_377 A_381 A_385 A_455 A_456 A_459 A_460 A_515 A_518 A_519 A_522 B_1427 B_1513 B_1516 B_1520
Pocket5	5	2.3	0.059	47	27	20.0955	7.7271	40.6197	A_459 A_464 A_468 A_469 A_472 A_473 A_476 B_1430 B_1433 B_1434 B_1437

Pocket6	6	1.44	0.019	33	15	30.7051	38.8326	35.1157	A_430 A_433 A_437 B_1459 B_1464 B_1469 B_1472 B_1476